



## 3D reconstruction of geological structures based on remote sensing data: example from Anaran anticline (Lurestan province, Zagros fold and thrust belt, Iran)

M. SNIDERO<sup>1</sup>\*, A. AMILIBIA<sup>1</sup>, O. GRATACOS<sup>1</sup> AND J. A. MUÑOZ<sup>1</sup>

<sup>1</sup>Geomodels research centre, GGAC, Dept. Geodinàmica i Geofísica, Facultat de Geologia, Universitat de Barcelona, 08028 Barcelona, Spain.

\*e-mail: msnidero@ub.edu

---

**Abstract:** This work describes a methodological workflow for the 3D reconstruction of geological surfaces, exclusively based on satellite data and regional-scale maps. A combined processing of Aster and SPOT images with a digital elevation model has been carried out in order to generate consistent 3D images on which our study is based. The structural data have been acquired by means of the 3D digital mapping. Applying the dip-domain methodology combined with the Discrete Smooth Interpolation (DSI) algorithm, the top surfaces of the Asmari and Ilam formations have been reconstructed along the southern Anaran anticline (Zagros fold and thrust belt mountain front). The reconstructed surface geometry allows us to classify the anticline as a fault propagation fold, clearly affected by a minor back-thrust.

**Keywords:** Zagros, 3D reconstruction, remote sensing, dip-domain, DSI.

---

The interest in 3D modelling comes from an attempt to be able to represent the geological reality, avoiding the crucial simplifications produced when working with 2D sections. The advantages and motivations of using 3D reconstruction instead of 2D section were extensively explained by Fernández *et al.* (2003). In the construction of a geological-structural 3D model, a uniform distribution of data along the structure should be ideal in order to adequately represent its geometrical variability. The availability of this distribution is restricted in areas of study located in regions with difficult access due to geographical or geopolitical reasons, like Iran. In order to solve this problem, we present a methodological workflow for 3D reconstruction of geological surfaces, on a regional scale, using remote sensing data and geological maps. The proposed methodology is based on the “dip-domain” concept, introduced in the first kink-style models of fault related folding (Coates, 1945; Gill, 1953;

Coward and Kim, 1981; Sanderson, 1982; Suppe, 1983; Jamison, 1987; Groshong, 1988), where every geological structure could be discretized in constant dip and azimuth volumes, bounded by surfaces with a geological sense (faults, axial planes, unconformities, etc.) (Fig. 1). The study area is the southern sector of the Anaran Anticline, located along the structural province of Lurestan Mountain Front, is part of the NE sector of the Simple Folded Belt structural unit that represents the external part of the Zagros fold and thrust belt (Fig. 2). Very characteristic large scale anticlines developed in this zone, spectacularly folding an up to 12-14 km-thick, mainly carbonate, sedimentary sequence (Falcon, 1974; Colman-Sadd, 1978; Blanc *et al.*, 2003). These structures have been classically interpreted as fault propagation and detachment folds (Sherkati *et al.*, 2005). The Anaran anticline is 100 km long and presents strong along-strike variations in structural style, geometry as well as

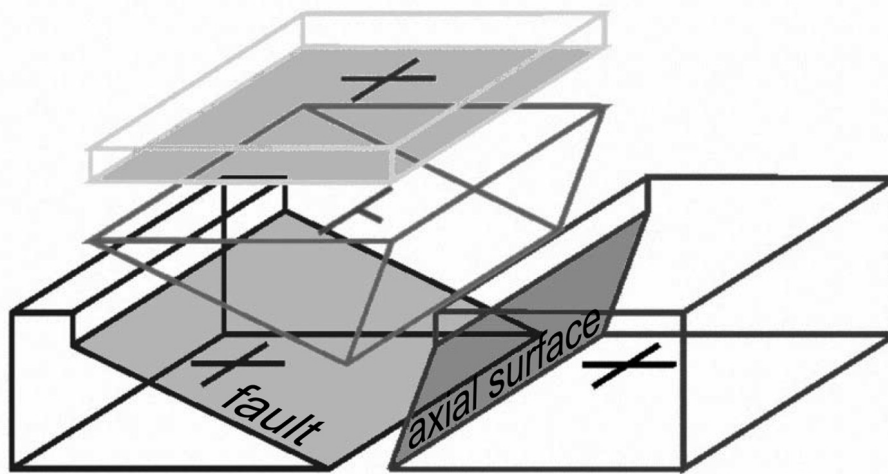


**Figure 1.** Dip-domain conceptual model. Dip-domains are represented by volumes with constant dip and azimuth and bounded by surfaces with geological significance (modified from Fernández *et al.*, 2004).

stratigraphic thickness. As a consequence, a three-dimensional approach is necessary to describe and understand the structure as well as its tectono-sedimentary evolution. The selected horizons for the 3D reconstruction of the anticline are the Asmari and Ilam formations tops. The selection of these horizons was based on their exploration importance as well as on their outcrop quality in order to get as much data as possible from the remote sensing images.

### Methodology

The structural data used for the surface reconstruction has been acquired from the 3D mapped geological traces on satellite images, as well as from the original geological maps of the area. The 3D image used for the 3D digital mapping has been obtained from panchromatic SPOT-HRG and Aster multi-band images draped on the stereoscopic SPOT-Dem. During this first methodological step the quality and consistency of the remote sensing dataset has been improved, increasing the spectral as well as the spatial resolution of the images. Aster images have been processed by the Optimum Index Factor (OIF) technique in order to obtain the maximum discrimination between the outcropping lithologies. Although the Normalized Difference Vegetation Index (NDVI) is the most widely used index, there are a few reports that demonstrate this index is not so effective in desertic areas (Pickup *et al.*, 1993; Ray and Murray, 1994). Among others, the OIF, based on total variance within bands and correlation coefficient between bands, is a statistical approach to rank all possible three-band combinations. The three-band combination with the biggest OIF value will have the maximum pixel variance and minimum amount of duplication (Ren and Abdelsalam, 2001). In this study, the combination

used was bands 3, 4 in the visible and near infrared (VNIR sensor, 15 m) and 6 short wave infrared (SWIR sensor, 30 m), characterized by high values of OIF, is the most reliable solution for an exhaustive lithology discrimination. In order to drastically increase the spatial resolution of the resulting image, it has been pansharpened with a 2.5 m resolution panchromatic Spot image. By doing so, the final result is a high resolution image with a good lithological differentiation by colours (Fig. 3a). Next step is the 3D mapping of the selected horizon over the produced 3D image, giving the related geological traces. From 3D mapped traces, and using the tools developed by Fernández *et al.*, (2004), we can calculate the plane that best fits the digitized points along the geological trace, extracting the new dip-data associated value. These will be the start dataset for the 3D reconstruction. Once the dataset has been obtained (Fig. 3b), dip-data are grouped in dip-domains with error ranging  $\pm 5^\circ$  in azimuth and  $\pm 3^\circ$  on dip. A mean plane is calculated for each dip-domain and projected to the proper stratigraphic position in order to reconstruct the selected horizons (Asmari and Ilam formations tops). At the same time, regional structural analysis is carried out, giving cylindrical domains along the anticline with their related plunge lines (Figs. 3b and 4). Using the plunge lines as vectors, dip domains have been projected along strike coherently with the geometrical model defined by the structural analysis (Fig. 4). This allowed us to supply data in the places where 3D mapping had not been fruitful. In the next step we define a boundary for every dip domain observing its fit with the relative geological trace. The dip-domains have been considered suitable only when the distance between the geological trace and the dip-domain main plane diverge no more than  $\pm 15$  m. The resultant planes (Fig. 3c) represent the frame of the structure. To

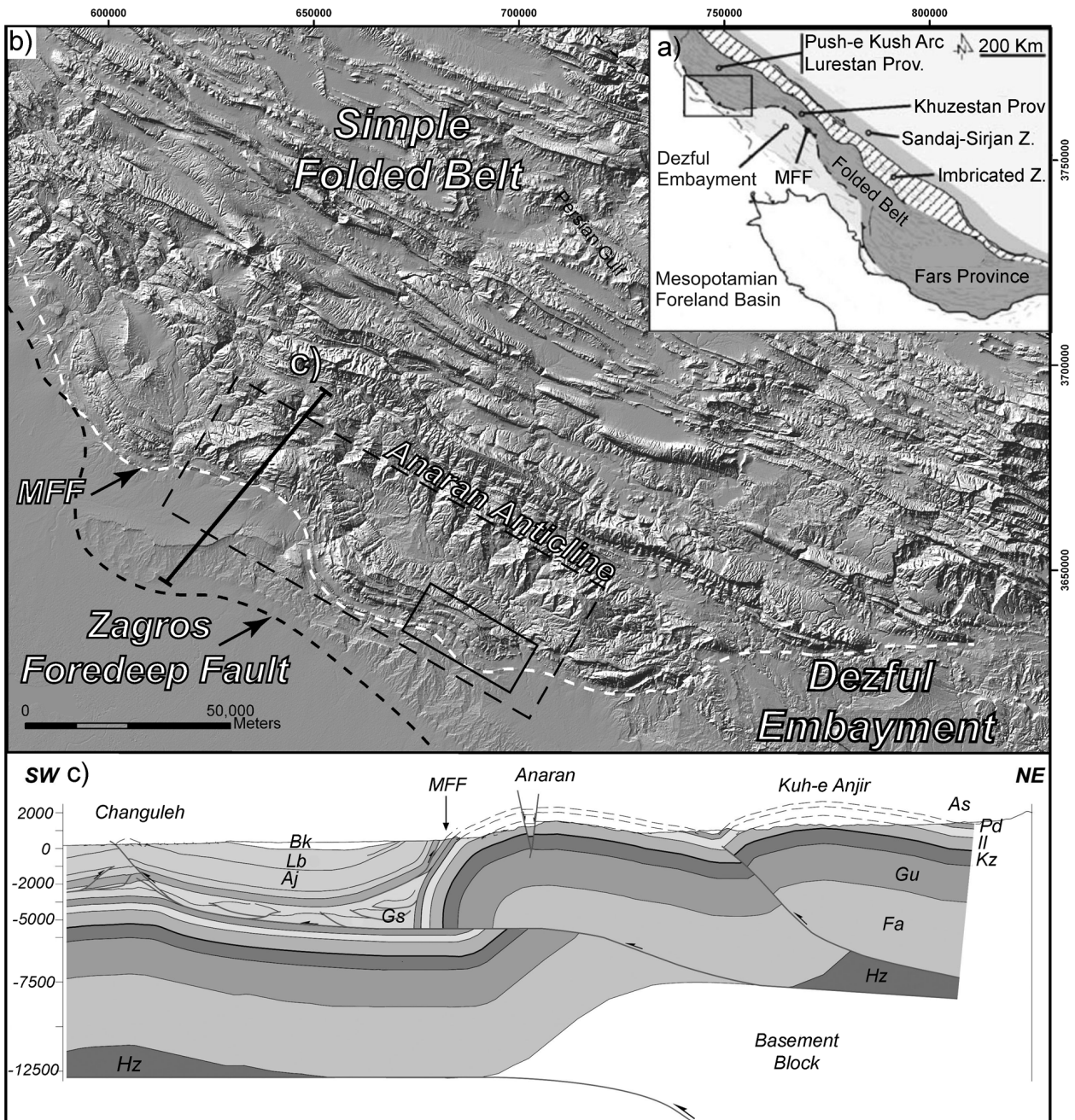


**Figure 2.** (a) Location of Lurestan Province in the Zagros fold and thrust belt, (b) hillshade model of Lurestan province DEM showing the main structural units and faults. Anaran anticline (dashed box) and the reconstructed section (solid line) are highlighted, (c) geological section across the southern Lurestan.

interpolate the surface between the obtained planes we use the Discrete Smooth Interpolator (DSI) (Mallet, 1992) implemented in Gocad® software. It uses a triangular mesh with an arbitrary set of nodes fixed by the user (constraints) and assigns coordinates to the other nodes of the mesh from multiple iterations, progressively reducing the sharpness of the final surface. Final Asmari and Ilam surfaces for the SE Anaran anti-

cline have been generated honouring the provided constrained data (Fig. 3d).

### Conclusions

The results so far, demonstrate that the proposed methodology is a powerful tool for 3D reconstruction of geological surfaces when working with remote

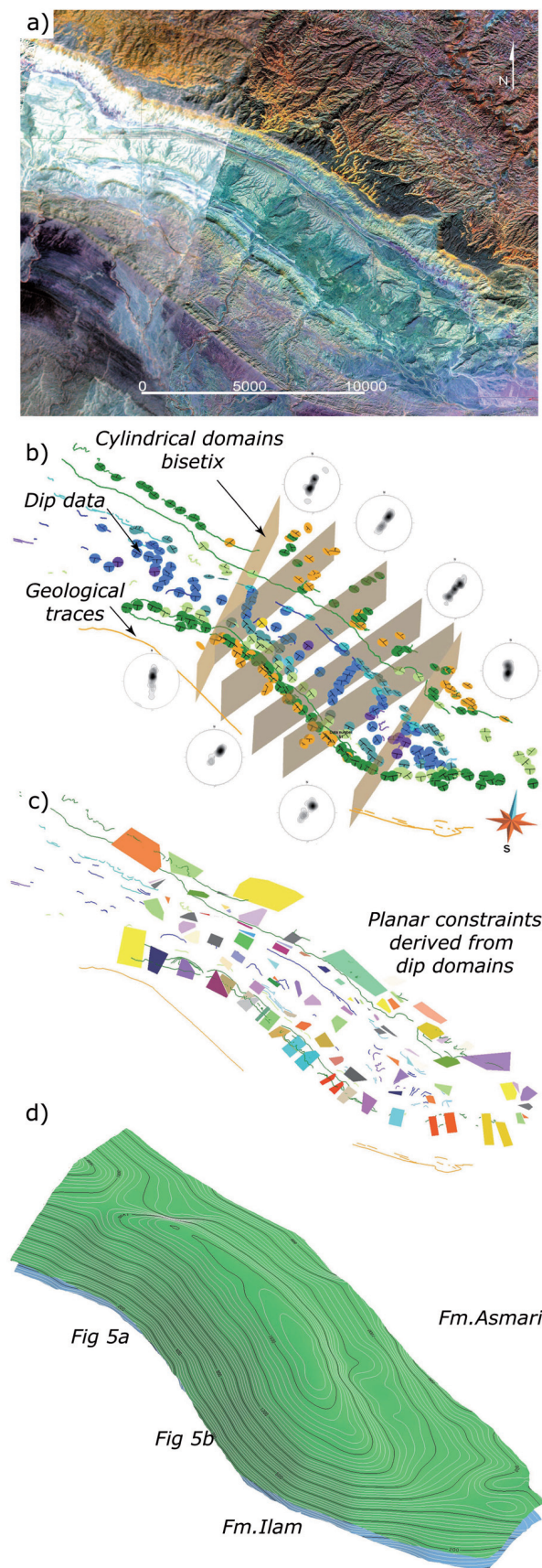


**Figure 3.** Methodological steps followed during 3D reconstruction. (a) Perspective view of the 3D image, composed by the processed satellite images draped on DEM, used for digital mapping, (b) mapped traces and dip dataset obtained. Cylindrical plots and bisector boundaries are also represented, (c) derived dip-domain main planes from dip dataset, projected to stratigraphic horizon. These planes will be the constraints for the 3D surface reconstruction, (d) final reconstructed surface of the Asmari an Ilam horizon (location of section shown in figure 5).

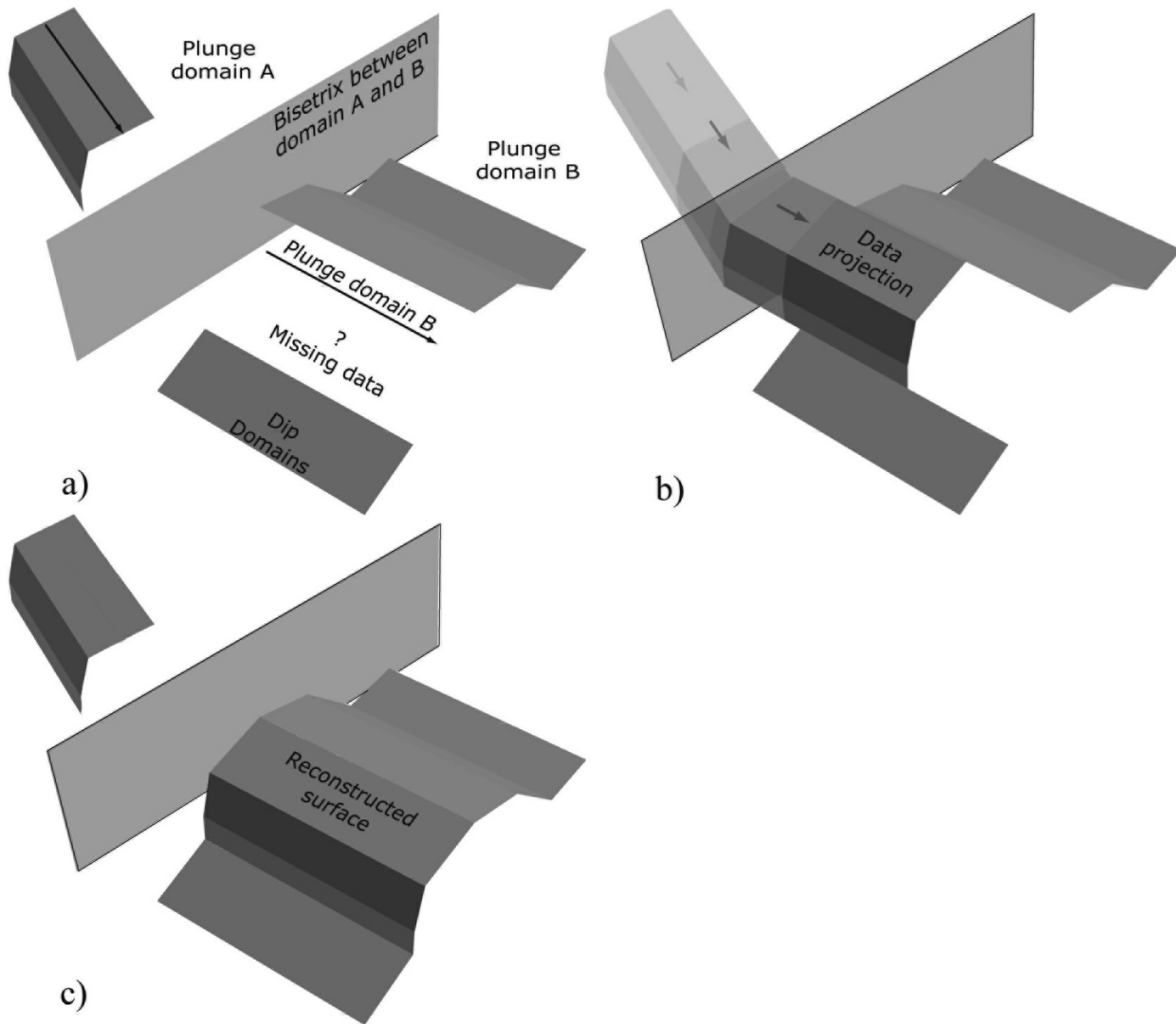


**Figure 4.** Dip-domain projection across cylindrical domains. (a) Initial theoretical dip-domain dataset showing gaps without available information. Plunge lines and bisector planes are also represented, (b) dip-domain projection from plunge domain A to plunge domain B in order to fill the information gap, (c) final dataset completed with projected data.

sensing data, in very inaccessible areas (e.g. Iran, China or Africa). It is especially useful in semiarid regions where the structure strongly controls the topography. It is also valid for preliminary studies previous to field work as well as for all the stages of exploration studies for the integration of surface and sub-surface data into a coherent structural model. The implementation of the DSI interpolation algorithm, strongly constrained to the structural data, allow us to obtain a major consistence between the final surfaces and the 3D mapped data. The reconstructed geometry of the fold surface shows the existence of four well-defined dip-domains: a frontal limb with an average slope of  $35^\circ$ , a sub-horizontal crest, an area with a

sub-vertical dip (in transit between the crest and the back limb), and by an extended back limb with an average slope of  $12^\circ$  (Fig. 5). The described geometry is coherent with a fault propagation fold model. Due to the constant altitude and vergence of the anticline crest, it is reasonable to assume that the fold thrust geometry is constant throughout the central sector of the reconstructed fold. The sub-vertical panel described has been interpreted as a back-thrust detached in the Surmeh formation, probably caused by the fold propagation blocking towards the fore-land, which itself is caused by the buttressing effect induced by the syn-tectonic sediments deposited in front of the structure.

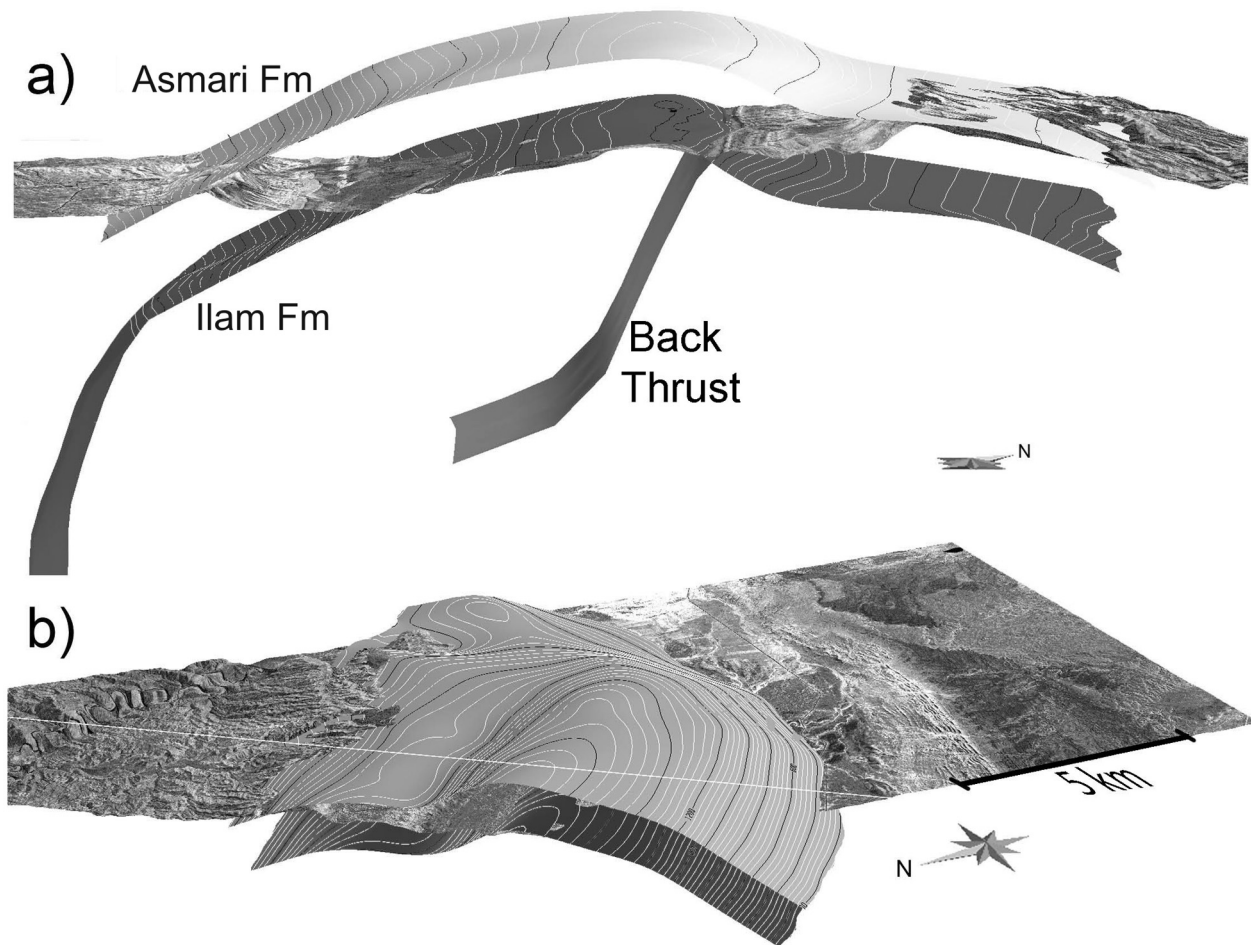


**Figure 5.** (a) Cross-section across the Anaran structure reconstructed surfaces (see location in figure 3d). a) Section a-a' across Anaran Anticline central sector. Notice the well-differentiated dip ranges, (b) 3D view of b-b' section of the Anaran Anticline southern closure.

### Acknowledgements

This work has been developed in the *Grupo de Geodinámica y Análisis de Cuencas*, and among the *Centre Mixt di Investigació*

### References

- BLANC, E. J. P., ALLEN, M. B., INGER, S. and ASAN, H. (2003): Structural styles in the Zagros Simple Folded Zone, Iran. *J. Geol. Soc. London*, 160, 3: 401-412.
- COATES, J. (1945): The construction of geologic sections. *Q. J. Geol. Min. Metall. Soc. India*, 17: 1-11.
- COLMAN-SADD, S. P. (1978): Fold development in Zagros Simply Folded Belt, southwest Iran. *AAPG Bull.*, 62: 984-1003.
- COWARD, M. P. and KIM, J. H. (1981): Strain within thrust sheets. In: K. R. McCLAY and N. J. PRICE (eds): *Thrust and Nappe Tectonics, Spec. Publ. Geol. Soc. London*, 9: 275-292.
- FALCON, N. L. (1974): Southern Iran: Zagros Mountains. In: A. SPENCER (ed): *Mesozoic-Cenozoic Orogenic Belts, Spec. Publ. Geol. Soc. London.*, 4: 199-211.
- FERNÁNDEZ, O., MUÑOZ, J. A. and ARBUÉS, P. (2003): Quantifying and correcting errors derived from apparent dip in the construction of dip-domain cross-sections. *J. Struct. Geol.*, 25: 35-42.
- FERNÁNDEZ, O., MUÑOZ, J. A., ARBUÉS, P., FALIVENE, O. and MARZO, M. (2004): Three-dimensional reconstruction of geological surfaces: An example of growth strata and turbidite systems from the Ainsa basin (Pyrenees, Spain). *AAPG Bull.*, 88: 1049-1068.
- GILL, W. D. (1953): Construction of geological sections of folds with steep-limb attenuation. *AAPG Bull.* 37: 2389-2406.
- GROSHONG, R. H. (1988): Low-Temperature deformation mechanisms and their interpretation. *Geol. Soc. Am. Bull.*, 100: 1329-1360.

- JAMISON, W. R. (1987): Geometric analysis of fold development in overthrust terranes. *J. Struct. Geol.*, 9: 207-219.
- MALLET, J. L. (1992): Discrete smooth interpolation in geometric modeling. *Computer-Aided Design*, 24, 4: 178-191.
- PICKUP, G., CHEWINGS, V. H. and NELSON, D. J. (1993): Estimating in change in vegetation in arid range land using Landsat MSS data. *Remote Sens. Environ.*, 43: 243-263.
- RAY, T. W. and MURRAY, B. C. (1994): Remote monitoring of shifting sands and vegetation cover in arid regions. In: W. JOBEA and D. MCCLEESE (eds): *IGARSS'94, International Geoscience and Remote Sensing Symposium; surface and atmospheric remote sensing; technologies, data analysis and interpretation*: 1033-1035.
- REN, D. and ABDELSALAM, M. G. (2001): Optimum Index Factor (OIF) for ASTER data; examples from the Neoproterozoic Allaqi Suture, Egypt. *Geol. Soc. Am.*, 33, 6: 289-290.
- SANDERSON, D. J. (1982): Models of strain variation in nappes and thrust sheets: a review. *Tectonophysics*, 88: 201-233.
- SHERKATI, S., MOLINARO, M., DE LAMOTTE, D. and LETOUZEY, J. (2005): Detachment folding in the Central and Eastern Zagros fold-belt (Iran): salt mobility, multiple detachments and late basement control. *J. Struct. Geol.*, 27: 1680-1696.
- SUPPE, J. (1983), Geometry and kinematics of fault-bend folding. *Am. J. Sci.*, 283: 684-771.